J Mater Sci (2019) 54:719–729

Materials for life sciences

Enhanced mechanical and osteogenic differentiation performance of hydroxyapatite/zein composite for bone tissue engineering

He Lian[1], Xue Liu[1], and Zhaoxu Meng[1,*]

[1] *Department of Biomedical Engineering, Faculty of Medical Instrument, Shenyang Pharmaceutical University, Shenyang 110016, China*

Received: 10 May 2018
Accepted: 10 August 2018
Published online: 17 August 2018

ABSTRACT

Herein, a series of hydroxyapatite (HAp)/zein biocomposite membranes, with different inorganic/organic weight ratios, are fabricated by solvent casting method by using ultra-long hydroxyapatite nanowires as the reinforcement. The FTIR spectra and XRD analysis of HAp/zein composite membrane confirm the structure of HAp nanowires and zein in composite membranes. When the HAp nanowires content increased from 50 to 90 wt%, the morphology of HAp/zein composite membrane transformed from the rough plane into the fibrous and porous structure, both Young's modulus and tensile strength exhibited about 40% of the increase, and the water absorption showed about 80% of improvement. Moreover, higher content of HAp nanowires improved the adhesion, proliferation and osteogenic differentiation of mouse bone marrow mesenchymal stem cells according to the examination of 3-(4,5-dimethylthiazol-2-yl)-2,5-diphenyltetrazolium bromide assay, alkaline phosphatase activity, calcium deposition and gene expression. The prepared HAp/zein 9/1 composite membrane is shown as a promising candidate for the bone repair and regeneration applications.

Introduction

The extracellular matrix (ECM), composed of a number of polysaccharides, proteins, proteoglycans and other substances, constitutes a complex network of cells attachment and growth [1–3]. In addition, the ECM plays a vital role in defining cell shape, structure, function, survival, proliferation, differentiation and migration, while maintaining all the physiological activities of the tissues or organs in their structure and function, such as immune response and wound healing [4]. Therefore, the effective simulation of ECM with appropriate materials is an eternal research topic in the area of tissue repair and reconstruction.

The hydroxyapatite (HAp) is the main component of hard tissues, such as bones and tooth, and offers excellent biocompatibility, osteoconduction and

Address correspondence to E-mail: mengzhaoxu2006@163.com

https://doi.org/10.1007/s10853-018-2796-0

osteoinduction. Hence, a number of HAp-containing materials have been used as a substitute for bone tissue repair and regeneration, which can be summarized in three categories: HAp-based ceramics, HAp-based coatings and HAp/polymer hybrids [5–10]. In particular, the HAp/polymer composites have garnered significant research attention due to the diverse nature of polymers. The synthetic polymers, such as PLGA and PCL, have excellent biodegradability, but lack of active sites and hydrophobicity limit their practical applications [11, 12]. In comparison, the natural polymers, such as collagen and chitosan, exhibit enhanced bioactivity and result in improved cell attachment, proliferation and growth [13, 14]. However, the composites of HAp and natural polymer demonstrate poor mechanical performance. Although the addition of a small amount of HAp nanocrystals improves the mechanical properties to a certain extent, there is still a considerable gap compared with the mechanical properties of hard tissues. The higher content of HAp results in aggregated nanocrystal and reduced mechanical performance [15, 16]. Therefore, the optimal amount of HAp crystals is required to obtain the desired level of mechanical performance.

Recently, a novel HAp nanowire, synthesized by a calcium oleate precursor solvothermal method, has been reported by Zhu's group [17–20]. The HAp nanowires have exhibited the length of hundred microns, excellent flexibility, biocompatibility and ability to form a paper with a certain strength [17]. The HAp nanowires, as reinforcement, are considered advantageous over other nanostructures due to the content-independent enhancement of mechanical properties and fibrous structure, which is similar to the ECM of bone tissue [18]. Therefore, we aimed to improve the mechanical properties of HAp/polymer composites by using HAp nanowires.

The selection of natural polymer is also important in designing optimal HAp/polymer hybrids. The protein as a natural polymer has been widely applied in bone repair and regeneration [21–23]. In comparison with those animal-sourced proteins, zein is a low-price plant-sourced protein, which is being rapidly developed in the biomedical field [24, 25]. Moreover, zein has shown favorable biocompatibility, resistant to microbial attack and biomineralization [26–28]. Hence, several zein-based composites have been explored and demonstrated enhanced attachment, proliferation and osteoblastic differentiation of marrow mesenchymal stem cells [29–31]. For instance, zein electrospun nanofibers, containing 5% HAp nanoparticles, were fabricated by Zhang et al. and exhibited excellent biocompatibility [31]. The HAp nanoparticles in the fiber contribute to the proliferation of human mesenchymal stem cells.

Herein, we developed a series of novel composite membranes, consisting of zein and HAp nanowires, to mimic the composition and microstructure of extracellular matrix, and characterized the morphology, thermal degradation, water absorption and mechanical properties. In addition, the influence on biocompatibility and osteogenic differentiation of marrow mesenchymal stem cells was investigated by ALP activity, calcium deposition and gene expression. The HAp/zein composite membranes have shown potential as a substitute for bone repair and regeneration.

Materials and methods

Materials

Zein, oleic acid, calcium chloride, sodium hydroxide, sodium dihydrogen phosphate dihydrate, oleic acid and *N*-hydroxysuccinimide (NHS) were purchased from Maya Chemical Reagent Co., Ltd (China). 1-[3-dimethylaminopropyl]-3-ethyl-carbodiimide hydrochloride (EDC) was obtained from Shanghai Haoran Biotechnology Co., Ltd (China).

Fabrication of composite membranes

The synthesis of hydroxyapatite nanowires was carried out by using a calcium oleate-based solvothermal method [17]. In a typical reaction, 7 mL of oleic acid, 4 mL of methanol and 9 mL of deionized water were mixed by stirring for 30 min. Then, 10 mL of $CaCl_2$ (0.16 M) aqueous solution, 10 mL of NaOH (1.75 M) aqueous solution and 10 mL of NaH_2PO_4 (0.22 M) aqueous solution were dropwise added into the above mixture and kept under continuous stirring for 30 min. The mixture was transferred into a Teflon-lined stainless steel autoclave (100 mL), which was sealed and heated at 180 °C for 24 h. After cooling down, the product was collected, washed, with ethanol and deionized water for three times, and dispersed in ethanol aqueous solution (70%) at 2 wt%.

Zein was dissolved in 70% ethanol solution, at a concentration of 2 wt%, and EDC/NHS (1:1) was added, as a cross-linking reagent, with 6 wt% of zein. Then, a series of composites with different ratios of HAp nanowires suspension and zein solution (9/1, 7/3 and 5/5) were mixed by ultrasonic dispersion and stirring. The HAp, zein and composite membranes were cast by separately transferring the HAp nanowires suspension, zein solution and mixtures into the Teflon dish, followed by drying at room temperature for 48 h.

Characterization

The HAp, zein and HAp/zein composite membranes were all coated with a thin layer of gold, and the morphology was observed by a scanning electron microscopy (SEM) (FE-SEM Model JSM-7011F, Japan). The structural analysis of membranes was carried out by FTIR and X-ray diffraction (XRD). The FTIR spectra were recorded by a Fourier transform infrared spectrophotometer (Nicolet iS5, USA), in the range of 400–4000 cm^{-1}, with a resolution of 4.0 cm^{-1}. The XRD spectra were collected by X-ray diffractometer (Bruker D8 Advance, Germany), equipped with the Cu-K_α source, at a scan rate of 4°/min.

Thermal behavior was studied by using a thermal gravimetric analyzer (TG 209 F1 Libra, Germany), ranging from room temperature to 800 °C, at a heating rate of 10 °C/min, under nitrogen flow.

For mechanical properties evaluation, the samples, conditioned in 50% humidity for 3 days, were cut into rectangular pieces (40 × 5 mm^2) and tested by using a uniaxial testing machine (Instron 3365), with a 100-N load cell at a crosshead speed of 5 mm/min. The thickness of the sample was measured with a micrometer having a precision of 1 μm. At least five samples were tested for each condition, and value was averaged out and reported here.

The water absorption was determined as follow: the samples (30 × 30 mm) were dried, weighed (W_1) and immersed in PBS (pH ~ 7.4) at room temperature for 24 h. Then, the samples were taken out, and surface water was removed. The samples were weighed (W_2) again, and the water absorption was calculated according to given formula:

$$\text{Water absorption}\,(\%) = (W_2 - W_1)/W_1 \times 100\% \quad (1)$$

Cell culture

The green fluorescent protein (GFP)-positive mouse bone marrow mesenchymal stem cells (MSCs) (Sidansai Biotechnology Company, China) were cultured in a α-modified minimum essential medium supplemented with 10% fetal bovine serum, 100 U/mL penicillin and 100 μg/mL streptomycin, in a humidified incubator at 37 °C with 5% CO_2. Then, HAp/zein composite and zein membranes were cut into small pieces (10 × 10 mm^2) and placed in the culture plate for sterilizing (UV irradiation for 48 h). The cells from the third passage were trypsinized and seeded in the plate with a density of 1×10^4 cell/well. The morphology of cells, on day 2, was observed by fluorescence microscopy (Mingmei MF30, China).

Cell proliferation

The proliferation of cells on the samples was measured by 3-(4,5-dimethylthiazol-2-yl)-2,5-diphenyltetrazolium bromide (MTT) assay. The cells were incubated in MTT (5 mg/mL) for 4 h, in 5% CO_2, at 37 °C on day 1, 3, 5 and 7. Then, 100 μL of sodium dodecyl sulfate (10% w/w SDS in 0.01 M HCl) was added in each well to dissolve the internalized purple formazan crystals. The absorbance was measured at 570 nm with a reference wavelength of 630 nm by a microplate reader (Bio-RAD 680, Bio-rad Co., USA).

Calcium deposition quantification

The cellular mineralization was measured as follows: Briefly, a series of calcium solution was added with ortho-cresolphthalein complexone and measured at 575 nm by using a microplate reader (Bio-RAD 680) to establish a standard curve. Then, the cells cultured for 7 and 14 days were separated and shaken in the dilute HCl solution for 6 h to dissolve the deposited mineral. Subsequently, the supernatant after centrifugation was taken out for measurement at 575 nm, and the calcium quantification was obtained from the standard curve.

Alkaline phosphatase (ALP) activity

The cells were washed by PBS (pH 7.4) for three times and detached with trypsin–EDTA. After lysing in 0.1% Triton X-100 by freezing and thawing for two

cycles, the reaction was started by adding p-nitrophenyl phosphate (pNpp) reaction solution for 30 min incubation at 37 °C and quenched by the addition of 1 M NaOH. The absorption was measured at 410 nm by using a microplate reader (Bio-RAD 680), and total protein content was measured by using a BCA protein assay kit (Sigma).

Gene expression

The associated osteogenic genes of collagen type I (COL I), runt-related transcription factor 2 (Runx2), osteocalcin and osteonectin of MSCs were measured on day 14. Total RNA was extracted from the cells cultured on HAp/zein composite membranes and reverse transcribed as per manufacturers' instructions. Then, the RT-PCR assays were carried out by a Real-Time PCR Systems (Applied Biosystems® 7500) as per given protocol: incubation at 95 °C for 2 min, 40 amplification cycles at 95 °C for 2 s, and annealing and extension at 60 °C for 5 s. The glyceraldehyde-3-phosphate dehydrogenase (GAPDH) was used as the internal control, gene expression was evaluated by the $2^{-\Delta\Delta CT}$ method, and primers are listed in Table 1. At least five species per sample were tested.

Statistical analysis

A software of origin 8.0 (Origin Lab Inc., USA) was used to analyze the obtained data. Values were averaged and expressed as mean ± standard deviation (SD).

Results

Morphology

The morphology of HAp nanowires, zein and HAp/zein composites is shown in Fig. 1. The zein membrane had a smooth surface, exhibiting an excellent film-forming property. In comparison, the HAp nanowires were easy to agglomerate in the cleaning process, so the surface roughness of the formed film after suction filtration was relatively large. The HAp nanowires, in HAp/zein 9/1 composite membrane, were randomly arranged and formed porous structures. The HAp/zein 7/3 composite membrane had a similar morphology to that of HAp/zein 9/1 composite membrane, but the porosity was obviously decreased due to the presence of higher zein content, which filled part of the pores among the nanowires. When the zein content reached 50 wt%, the HAp nanowires were all covered by zein without any pores and only traces of nanowires were observed on the membrane surface.

FTIR spectrum

The FTIR spectra of HAp nanowires, zein and HAp/zein composite membranes are shown in Fig. 2. The characteristic peaks of HAp nanowires, such as the asymmetric and symmetric stretching vibration of phosphate at 1088 and 1015 cm^{-1} and the bending vibration of the O–P–O bond of the phosphate at 630, 598 and 556 cm^{-1}, were observed in the spectra of HAp/zein composites [32, 33]. The amide I (1651 cm^{-1}) and amide II (1546 cm^{-1}) of zein protein were also present in the composite membranes [34]. The intensity of these peaks was proportional to the composition of HAp nanowires and zein protein.

XRD patterns

Figure 3 presents the XRD patterns of HAp/zein composite membranes, which are similar to HAp nanowires. The prominent diffraction peaks at 10.7°, 29.0°, 31.8°, 33.0°, 39.9°, 50.4°, 51.4° and 59.9° correspond to the crystal faces of (100), (210), (211), (300), (310), (321), (410) and (420) of HAp, respectively (JCPDF file No. 09-0432). However, the weak peaks, present at 42.0° and 46.7°, corresponding to the HAp crystal faces of (311) and (222), were decreased with

Table 1 RT-PCR primers for indicated genes

Gene	Primer sequence (5′–3′)	
	Forward	Reverse
COL I	AGCGAAGAACTCATACAGCCG	TGCCCGTCTCCTCATCCA
Runx2	CTTCACAAATCCTCCCCAAGT	AGGCGGTCAGAGAACAAACTA
Osteocalcin	AAGCAGGAGGGCAATAAGGT	TTTGTAGGCGGTCTTCAAGC
Osteonectin	AGGTATCTGTGGGAGCTAATC	ATTGCTGCACACCTTCTC

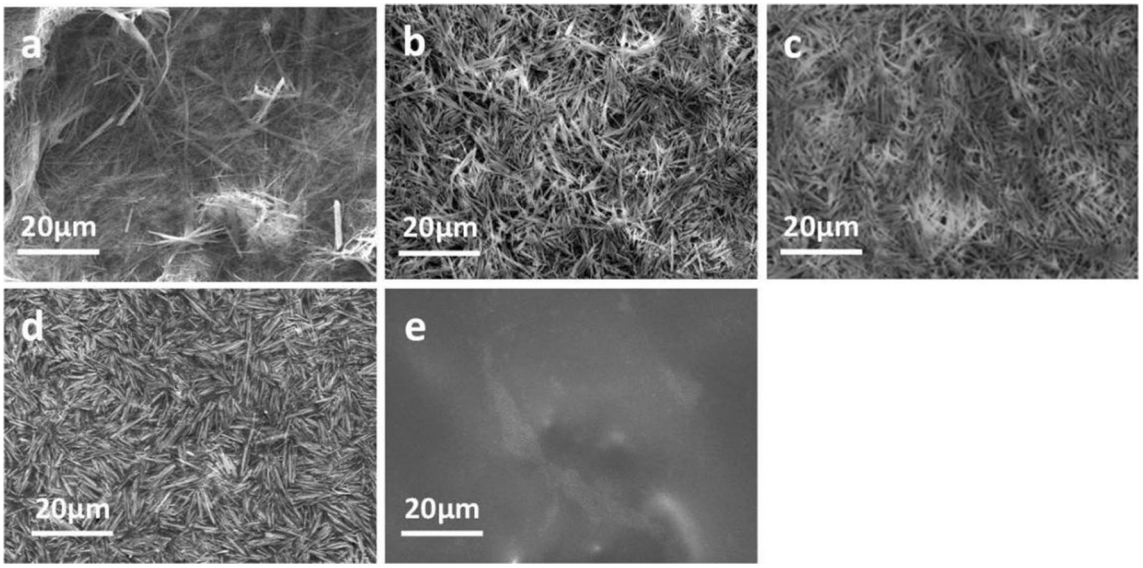

Figure 1 The morphology of HAp nanowire membrane (**a**), HAp/zein composite membranes (**b**: 9/1, **c**: 7/3, **d**: 5/5), and zein membrane (**e**).

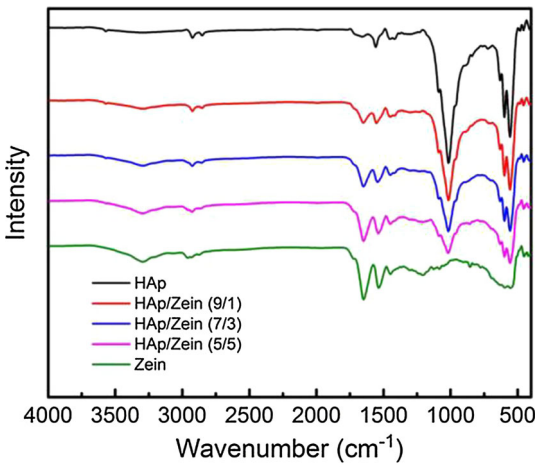

Figure 2 FTIR spectrum of HAp nanowires, zein and HAp/zein composite membranes.

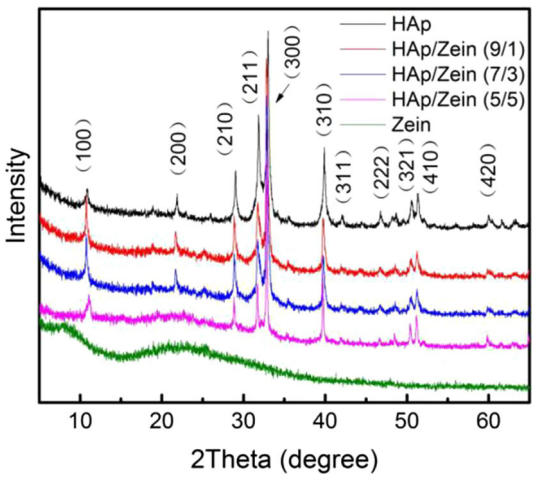

Figure 3 XRD patterns of HAp nanowires, zein and HAp/zein composite membranes.

the increase in zein protein [35]. Furthermore, the (200) peak of HAp was greatly influenced by the broad peak of zein protein (~ 22°), when the zein content reached 50 wt%.

Thermal analysis

The thermal degradation of the composites was measured by thermo-gravimetric analysis (TGA), and results are presented in Fig. 4. The weight loss of HAp nanowires was about 1.36%, which might be due to the adsorbed water from the air or residual organic matters. The curve of zein membrane exhibited two steps, separated by about 220 °C, similar to the published reports [36, 37]. The first stage (room temperature ~ 220 °C) corresponds to the water evaporation, and the second stage (220–600 °C) indicates the decomposition of zein. The HAp/zein composites had shown the similar trend, and the residue weight was 87.22, 68.24 and 49.59% for HAp/zein 9/1, 7/3 and 5/5 membranes, respectively. The residue of the HAp/zein composite membrane has shown a small increase with higher zein content, which is attributed to the fact that higher zein content has filled the pores of the

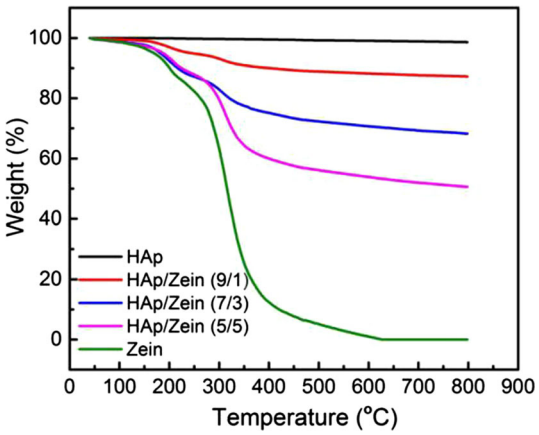

Figure 4 TGA curves of HAp nanowires, zein and HAp/zein composite membranes.

composite membrane and reduced water absorption (Fig. 1b–d).

Water absorption

The result of water absorption of zein and HAp/zein composite membranes is shown in Fig. 5. It can be readily observed that the zein membrane has shown the water absorption of only 22%. However, the addition of HAp nanowires has increased the water absorption ability, and the HAp/zein 9/1 composite membrane has absorbed five times more water than pure zein.

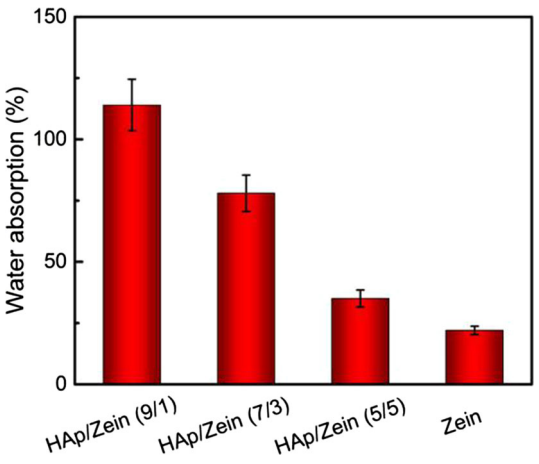

Figure 5 Water absorption of zein and HAp/zein composite membranes.

Mechanical property

The mechanical performance is critical in determining the practical utilization of these membranes in bone tissues. The Young's modulus, tensile stress and elongation at breakage point are listed in Table 2. Among tested membranes, the HAp/zein composite membrane of 9/1 exhibited the maximum Young's modulus and tensile strength of 1.01 ± 0.13 GPa and 89.17 ± 4.52 MPa, respectively.

Cell adhesion and proliferation

The cells were seeded on the surface of HAp/zein composite membrane, and the cell adhesion and proliferation are shown in Fig. 6. We have not observed a significant difference during first 3 days. However, the cell number on HAp/zein 9/1 and 7/3 composite membranes was higher than that of HAp/zein 5/5 composite membrane and zein membrane ($p < 0.05$). The fluorescent photographs showed that the cells were evenly distributed on the membrane surface, normal in shape, and showed a spreading state (Fig. 7).

ALP activity

The ALP activity of MSCs on the HAp/zein composite and zein membranes was measured, on day 7 and day 14, to examine the osteogenic differentiation of cells (Fig. 8). It has been observed on day 7 that the ALP level decreased with the addition of zein and a significant difference existed between the four groups. However, on day 14, quite obvious differences were observed between the five groups, and ALP activity of cells on HAp/zein 9/1 was still the highest in the groups.

Cellular mineralization

The calcium ions came from the minerals deposited on the cell surface, which was also an indicator of osteogenic differentiation of MSCs. Figure 9 shows the calcium ion concentration to characterize the cellular mineralization of cells on HAp/zein composite membranes. The significant difference occurred between the groups on both day 7 and 14, and the calcium minerals from cells on HAp/zein composite membrane were increased with increasing of HAp nanowires.

Table 2 Mechanical property of zein and HAp/zein composite membranes

Sample	Young's modulus (GPa)	Tensile stress (MPa)	Elongation at break (%)
HAp/zein 9/1	1.01 ± 0.13	89.17 ± 4.52	4.76 ± 1.02
HAp/zein 7/3	0.89 ± 0.16	79.26 ± 6.01	7.11 ± 1.98
HAp/zein 5/5	0.66 ± 0.42	51.02 ± 4.71	12.25 ± 2.38
Zein	0.54 ± 0.09	39.58 ± 8.09	18.26 ± 6.42

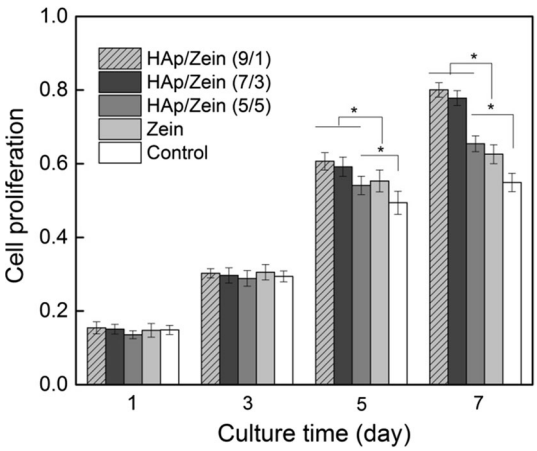

Figure 6 Cell adhesion and proliferation on zein and HAp/zein composite membranes (*$p < 0.05$).

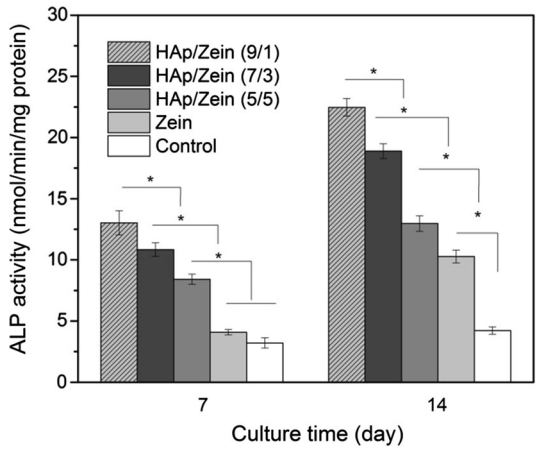

Figure 8 ALP activity of the MSCs cultured on HAp/zein composite membranes for 7 and 14 days (*$p < 0.05$).

Gene expression

Figure 10 displays the expression of gene related to osteogenic differentiation of MSCs. COL I, Runx2, osteonectin and osteocalcin were evaluated by RT-PCR on day 14. The cells on HAp/gelatin 9/1 composite membrane always showed highest level of gene expression; however, the lowest level of gene expression appeared on zein membrane.

Discussion

In this paper, we intend to mimic the extracellular matrix of the bone, both in composition and structure, to fabricate a novel substitute for bone repair

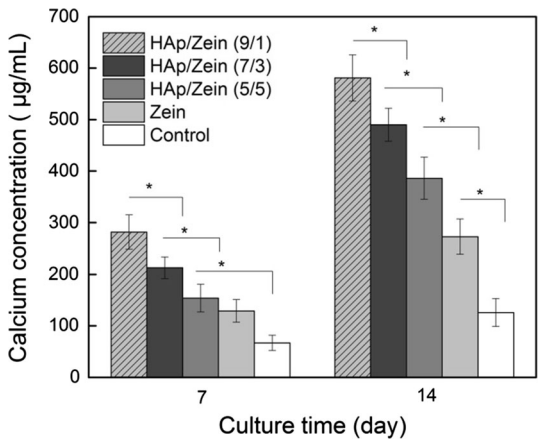

Figure 9 Cellular mineralization of the MSCs cultured on HAp/zein composite membranes for 7 and 14 days (*$p < 0.05$).

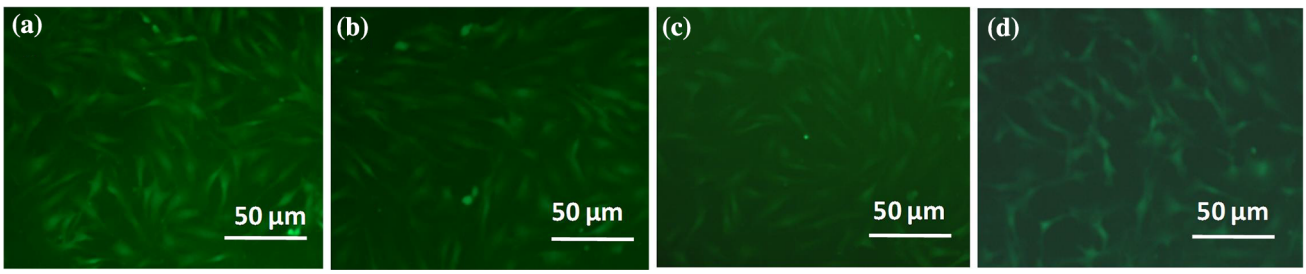

Figure 7 Fluorescent images of MSCs on HAp/zein composite membranes (**a**: 9/1, **b**: 7/3, **c**: 5/5, **d**: zein).

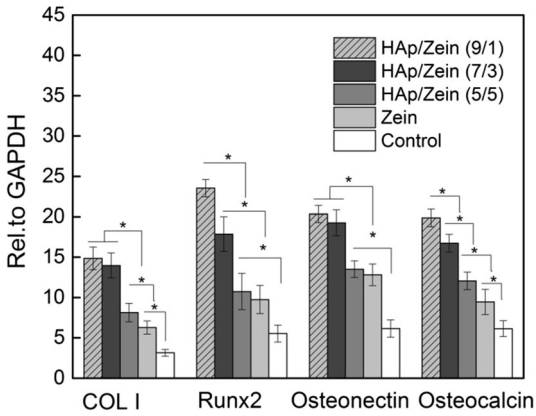

Figure 10 Gene expression of MSCs cultured on HAp/zein composite membranes for 14 days (*$p < 0.05$).

and regeneration with suitable components, structure, mechanical performance and osteoinductive. The ECM was a network for cell adhesion and proliferation, so the fibrous microstructure of the substitute is favorable. In our previous works, we have utilized nanofibrous membrane, prepared by electrospinning, as a matrix to mimic the ECM structure for bone cells [38, 39]. However, the major drawback was that the composition of electrospun nanofibrous membranes could not simulate the composition of the bone. The main component of bone was hydroxyapatite (70 wt%), but HAp nanocrystal incorporated into electrospun fibers could not reach this level [38]. Additionally, the satisfactory surface mineralization and optimum mechanical performance were still not obtained [39].

The appearance of ultra-long HAp nanowires provided a new choice for the preparation of substitute for bone tissue [17–20]. In this case, we have chosen ultra-long HAp nanowires, as the main inorganic component, and zein, as the organic component, to prepare a novel substitute for bone repair and regeneration. The HAp nanowires possess excellent flexibility and form a fibrous structure with high porosity, which was similar to the ECM of the bone [17]. In addition, the HA nanowires were bundled, overlapped and intertwined with each other, leading to a higher interaction between the HAp nanowires and thus enhancing the mechanical property of the substitute. As a hydrophobic protein, zein has a low water absorption rate and degradation rate and can maintain the shape and mechanical property for a long time. In addition, it is positive to the mineralization of phosphorus and calcium ions, so it has recently developed rapidly in bone tissue engineering [40–42].

In order to find optimal composition, we have prepared a series of HAp/zein composite membranes consisting of ultra-long HAp nanowires and zein. It was shown that the HAp/zein 9/1 and 7/3 exhibited fibrous and porous microstructure in the membranes (Fig. 1), whereas the pores were filled up when zein content reached up to 50 wt%. Therefore, the HAp/zein 9/1 and 7/3 composite membranes are suitable candidates from the compositional and structural viewpoint. It has been observed that the zein had a low swelling ratio in comparison with other natural materials, such as collagen, silk and chitosan (Fig. 5), which is beneficial for a bone substitute because the higher swelling leads to the larger deformation and inferior mechanical performance. The mechanical performance had always been a key concern for porous materials because the presence of pores undermines the continuity of the material and increases the crack initiation and propagation sites [43]. Hence, a compromise between the porosity and mechanical properties of biomaterials remained a challenging task to the researchers so far. Herein, the porous HAp/zein composite membrane exhibited higher tensile strength and Young's modulus than that of zein membrane, owing to the self-assembled, intertwined and bundled HAp nanowires combined with the interaction of zein chains. In addition, the elongation of the composite was still higher than natural bone (> 2%) [44]. Therefore, the HAp/zein 9/1 composite membrane demonstrated desired morphological, structural and mechanical behavior.

As a substitute for bone tissue, the cell response also plays a critical role because the substitute would provide an environment for cell attachment, proliferation and differentiation. Currently, the induction of osteogenic differentiation of MSCs drew more attention because the MSC, as a seed cell, can differentiate into osteoblasts under different inducing conditions [45–48]. In this work, we have evaluated the ALP activity, calcium deposition and gene expression of MSCs on different HAp/zein composite membranes, which are typical markers during the osteogenic differentiation of MSCs. The results indicated that the content of HAp nanowires contributed to the osteogenic differentiation of MSCs and HAp/zein 9/1 composite membrane had shown excellent osteogenic differentiation performance among the composites. It has been reported that the composition

and structure of the material have a certain influence on the osteoinduction [47, 48]. The HAp/zein 9/1 composite exhibited fibrous and porous structure which was similar to that of ECM of bone, which would attribute to the cell proliferation. In addition, the release of Ca and P ions from HA nanowires is the important factor in the control of osteogenesis [49, 50]. The concentration of Ca and P ions increased with increasing HA nanowire content and culture time, leading to greater osteogenic differentiation of MSCs on composites with a higher HA nanowire content. Based on above results, the HAp/zein 9/1 composite membrane is a suitable candidate for bone repair and regeneration applications due to its enhanced both cells proliferation and differentiation.

Conclusions

In this study, we have developed a novel HAp/zein composite membrane, which is a potential substitute for hard tissue in bone repair and regeneration applications. The higher content of HAp nanowires contributed to improve fibrous microstructure, enhance mechanical properties and stimulate the osteogenic differentiation of MSCs, according to the results of ALP activity, calcium deposition and gene expression. The HAp/zein 9/1 composite membrane exhibited excellent morphological, structural and mechanical properties.

Acknowledgements

This work is supported by National Natural Science Foundation of China (Nos. 31600764, 81503020), Scientific Research Project of Liaoning Provincial Department of Education (Nos. 2017LQN10, 201610163L27), the Science and Technology Project of Shenyang City (No. 18-013-0-47) and College Students Innovation and Entrepreneurship Project (1710163000159).

Compliance with ethical standards

Conflict of interest No conflict of interest exists in the submission of this manuscript, and manuscript is approved by all authors for publication.

References

[1] Wang Q, Xu J, Jin H, Zheng W, Zhang X, Huang Y, Qian Z (2017) Artificial periosteum in bone defect repair—a review. Chin Chem Lett 28:1801–1807

[2] Chan XY, Eoh JH, Gerecht S (2018) Let's get physical: biomechanical influences on human pluripotent stem cell differentiation towards vascular engineering. Curr Opin Biomed Eng 5:42–49

[3] Nissar AA, Martowirogo A, Gilbert PM (2016) Targeting the stem cell niche with regenerative biomaterials. Curr Opin Solid State Mater Sci 20:180–192

[4] Agmon G, Christman KL (2016) Controlling stem cell behavior with decellularized extracellular matrix scaffolds. Curr Opin Solid State Mater Sci 20:193–201

[5] Guillaume O, Geven MA, Sprecher CM et al (2017) Surface-enrichment with hydroxyapatite nanoparticles in stereolithography-fabricated composite polymer scaffolds promotes bone repair. Acta Biomater 54:386–398

[6] Mbarki M, Sharrock P, Fiallo M, ElFeki H (2017) Hydroxyapatite bioceramic with large porosity. Mater Sci Eng C 76:985–990

[7] Shen X, Zhang Y, Gu Y, Xu Y, Liu Y, Li B, Chen L (2016) Sequential and sustained release of SDF-1 and BMP-2 from silk fibroin-nano hydroxyapatite scaffold for the enhancement of bone regeneration. Biomaterials 106:205–216

[8] Mao D, Li Q, Bai N, Dong H, Li D (2018) Porous stable poly(lactic acid)/ethyl cellulose/hydroxyapatite composite scaffolds prepared by a combined method for bone regeneration. Carbohydr Polym 180:104–111

[9] Sukul M, Min YK, Lee BT (2016) Collagen-hydroxyapatite coated unprocessed cuttlefish bone as a bone substitute. Mater Lett 181:156–160

[10] Hajinasab A, Saber-Samandari S, Ahmadi S, Alamara K (2018) Preparation and characterization of a biocompatible magnetic scaffold for biomedical engineering. Mater Chem Phys 204:378–387

[11] Xin X, Guan Y, Yao S (2018) Bi-/multi-modal pore formation of PLGA/hydroxyapatite composite scaffolds by heterogeneous nucleation in supercritical CO_2 foaming. Chin J Chem Eng 26:207–212

[12] Qian J, Xu M, Suo A, Yang T, Yong X (2012) An innovative method to fabricate honeycomb-like poly(ε-caprolactone)/nano-hydroxyapatite scaffolds. Mater Lett 93:72–76

[13] Balagangadharan K, Dhivya S, Selvamurugan N (2017) Chitosan based nanofibers in bone tissue engineering. Int J Biol Macromol 104:1372–1382

[14] Basha RY, Kumar TSS, Doble M (2015) Design of biocomposite materials for bone tissue regeneration. Mater Sci Eng C 57:452–463

[15] Navarro-Baena I, Arrieta MP, Sonseca A et al (2015) Biodegradable nanocomposites based on poly(ester-urethane) and nanosized hydroxyapatite: plastificant and reinforcement effects. Polym Degrad Stab 121:171–179

[16] Kim H, Che L, Ha Y, Ryu WH (2014) Mechanically-reinforced electrospun composite silk fibroin nanofibers containing hydroxyapatite nanoparticles. Mater Sci Eng C 40:324–335

[17] Lu BQ, Zhu YJ, Chen F (2014) Highly flexible and nonflammable inorganic hydroxyapatite paper. Chem Eur J 20:1242–1246

[18] Hu J, Zhu Y, Tong H, Shen X, Chen L, Ran J (2016) A detailed study of homogeneous agarose/hydroxyapatite nanocomposites for load-bearing bone tissue. Int J Biol Macromol 82:134–143

[19] Chen F, Zhu YJ (2016) Large-scale automated production of highly ordered ultralong hydroxyapatite nanowires and construction of various fire-resistant flexible ordered architectures. ACS Nano 10:11483–11495

[20] Yang RL, Zhu YJ, Chen FF, Dong LY, Xiong ZC (2017) Luminescent, fire-resistant, and water-proof ultralong hydroxyapatite nanowire-based paper for multimode anticounterfeiting applications. ACS Appl Mater Interfaces 9:25455–25464

[21] Ding L, Li X, Sun H et al (2014) Transplantation of bone marrow mesenchymal stem cells on collagen scaffolds for the functional regeneration of injured rat uterus. Biomaterials 3:4888–4900

[22] Echave MC, Sánchez P, Pedraz JL, Orive G (2017) Progress of gelatin-based 3D approaches for bone regeneration. J Drug Deliv Sci Technol 42:63–74

[23] Farokhi M, Mottaghitalab F, Samani S et al (2018) Silk fibroin/hydroxyapatite composites for bone tissue engineering. Biotechnol Adv 36:68–91

[24] Cui H, Liu GL, Padua GW (2016) Cell spreading and viability on zein films may be facilitated by transglutaminase. Colloid Surf B 145:839–844

[25] Paliwal R, Palakurthi S (2014) Zein in controlled drug delivery and tissue engineering. J Control Release 189:108–122

[26] Wang GW, Yang H, Wu WF, Zhang P, Wang JY (2017) Design and optimization of a biodegradable porous zein conduit using microtubes as a guide for rat sciatic nerve defect repair. Biomaterials 131:145–159

[27] Reddy N, Yang Y (2011) Potential of plant proteins for medical applications. Trends Biotechnol 29:490–498

[28] Qu ZH, Wang HJ, Tang TT, Zhang XL, Wang JY, Dai KR (2008) Evaluation of the zein/inorganics composite on biocompatibility and osteoblastic differentiation. Acta Biomater 4:1360–1368

[29] Tu J, Wang H, Li H, Dai K, Wang J, Zhang X (2009) The in vivo bone formation by mesenchymal stem cells in zein scaffolds. Biomaterials 30:4369–4376

[30] Wu F, Wei J, Liu C, O'Neill B, Ngothai Y (2012) Fabrication and properties of porous scaffold of zein/PCL biocomposite for bone tissue engineering. Compos Part B Eng 43:2192–2197

[31] Zhang M, Liu Y, Jia Y, Han H, Sun D (2014) Preparation and evaluation of electrospun zein/HA fibers based on two methods of adding HA nanoparticles. J Bionic Eng 11:115–124

[32] Kebiroglu MH, Orek C, Bulut N, Kaygili O, Keser S, Ates T (2017) Temperature dependent structural and vibrational properties of hydroxyapatite: a theoretical and experimental study. Ceram Int 43:15899–15904

[33] Malakauskaite-Petruleviciene M, Stankeviciute Z, Niaura G, Garskaite E, Beganskiene A, Kareiva A (2016) Characterization of sol–gel processing of calcium phosphate thin films on silicon substrate by FTIR spectroscopy. Vib Spectrosc 85:16–21

[34] Han YL, Xu Q, Lu ZQ, Wang JY (2014) Preparation of transparent zein films for cell culture applications. Colloid Surf B 120:55–62

[35] Türk S, Altınsoy İ, ÇelebiEfe G, Ipek M, Özacar M, Bindal C (2017) Microwave-assisted biomimetic synthesis of hydroxyapatite using different sources of calcium. Mater Sci Eng C 76:528–535

[36] Neo YP, Swift S, Ray S, Gizdavic-Nikolaidis M, Jin J, Perera CO (2013) Evaluation of gallic acid loaded zein submicron electrospun fibre mats as novel active packaging materials. Food Chem 141:3192–3200

[37] Chen Y, Ye R, Li X, Wang J (2013) Preparation and characterization of extruded thermoplastic zein–poly(propylene carbonate) film. Ind Crop Prod 49:81–87

[38] Meng ZX, Wang YS, Ma C, Zheng W, Li L, Zheng YF (2010) Electrospinning of PLGA/gelatin randomly-oriented and aligned nanofibers as potential scaffold in tissue engineering. Mater Sci Eng C 30:1204–1210

[39] Meng ZX, Li HF, Sun ZZ, Zheng W, Zheng YF (2013) Fabrication of mineralized electrospun PLGA and PLGA/gelatin nanofibers and their potential in bone tissue engineering. Mater Sci Eng C 33:699–706

[40] Ru JY, Wei Q, Yang LQ, Qin J, Tang LC, Wei J, Guo LP, Niu YF (2018) Zein regulating apatite mineralization, degradability, in vitro cells responses and in vivo osteogenesis of 3D-printed scaffold of n-MS/ZN/PCL ternary composite. RSC Adv 8:18745–18756

[41] Tran PHL, Tran TTD, Nguyen MNU, Vo TV (2017) Zein-based solid dispersion for potential application in targeted delivery. J Pharm Investig 47:357–364

[42] Corradini E, Curti PS, Meniqueti AB, Martins AF, Rubira AF, Muniz EC (2014) Recent advances in food-packing, pharmaceutical and biomedical applications of zein and zein-based materials. Int J Mol Sci 15:22438–22470

[43] Ullah S, Zainol I, Chowdhury SR, Fauzi MB (2018) Development of various composition multicomponent chitosan/fish collagen/glycerin 3D porous scaffolds: effect on morphology, mechanical strength, biostability and cytocompatibility. Int J Biol Macromol 111:158–168

[44] Yamada H (1970) Strength of biological material. The Williams & Wilkins Company, Baltimore, pp 19–27

[45] Kanda Y, Nishimura I, Sato T, Katayama A, Arano T, Ikada Y, Yoshinari M (2016) Dynamic cultivation with radial flow bioreactor enhances proliferation or differentiation of rat bone marrow cells by fibroblast growth factor or osteogenic differentiation factor. Regen Ther 5:17–24

[46] Okada H, Takahashi K, Ogura N, Tomoki R, Ito K, Kondoh T (2016) Plasma rich in growth factors stimulates proliferation, migration, and gene expression associated with bone formation in human dental follicle cells. J Dent Sci 11:245–252

[47] Patel AK, Tibbitt MW, Patelab AK et al (2016) High throughput screening for discovery of materials that control stem cell fate. Curr Opin Solid State Mater Sci 20:202–211

[48] Hilderbrand AM, Ovadi EM, Rehmann MS, Kharkar PM, Guo C, Kloxin AM (2016) Biomaterials for 4D stem cell culture. Curr Opin Solid State Mater Sci 20:212–224

[49] Danoux CBSS, Bassett DC, Othman Z, Rodrigues AI, Reis RL, Barralet JE, van Blitterswijk CA, Habibovic P (2015) Elucidating the individual effects of calcium and phosphate ions on hMSCs by using composite materials. Acta Biomater 17:1–15

[50] Malhotra A, Habibovic P (2016) Calcium phosphates and angiogenesis: implications and advances for bone regeneration. Trends Biotechnol 34:983–992